# Synthesis of Scan and Frequency Invariant Low-Sidelobe Tapers for Planar Array Antennas

W. P. M. N. Keizer, *Member, IEEE*

***Abstract*—The impact of the array factor on the synthesis of a low sidelobe taper for planar array antennas with a periodic element grid is investigated. A low sidelobe taper that is synthesized for those far-field directions of the array factor belonging to only visible direction cosine u-v space, can seriously deteriorate with respect to peak sidelobe level when the main beam is scanned or the operating frequency is raised. In order to get a scan and frequency invariant taper, its synthesis must comprise all far-field directions of the array factor including those of invisible u-v space. This communication describes the Fourier properties that are responsible for the degradation of taper sidelobe level performance when the taper synthesis excludes the invisible space region of the array factor. Examples are presented for a circular array antenna to illustrate the impact of the invisible region of the array factor on sidelobe performance. The presented results refer to both phase-only and amplitude-only sidelobe tapers. The condition to realize for aperiodic planar array antennas scan and frequency proof patterns with invariant peak side lobe level is shortly addressed.**

***Index Terms*—Low sidelobe synthesis, array factor, periodic planar array antennas, visible space, scanning.**

## I. Introduction

The array factor (AF) of a planar array featuring a rectangular element grid will extend into invisible u-v space for an element spacing less than a halve wavelength. The direction cosine parameters u and v are defined by $u = sin\theta cos\varphi$ and $= sin\theta sin\varphi$ where are $\theta$ and $\varphi$ the angular coordinates of the far-field direction. Invisible u-v space covers the spectrum $u^2 + v^2 > 1$ and visible space is defined by the region $u^2 + v^2 \leq 1$.

The synthesis of a low sidelobe taper restricted to far-field directions inside visible u-v space while AF extends into invisible space, will in general not reveal a taper that is scan and frequency proof with respect to peak sidelobe level (PSLL). A taper applied to an array antenna equipped with isotropic radiators, is considered scan and frequency proof when its PSLL performance is invariant with scan angle and frequency.

Keeping out the invisible u-v space part of AF from low sidelobe taper synthesis, will have as consequence that a high PSLL levels in this region cannot be excluded. Since this region will enter visible u-v space when the scanning the main beam or raising the operating frequency, a decline of the PSLL is therefore very likely.

Since the AF of a planar array antenna represents a finite 2-D Fourier series, a number of Fourier properties apply to it. Two Fourier properties are discussed that are responsible for a likely PSLL increase when the beam is scanned or the operating frequency is raised. Representative examples are given for phase-only low sidelobe tapers synthesized for a circular array antenna using a rectangular element grid.

As far as is known by this author, this is the first time in open literature that the impact of the array factor on the synthesis of low sidelobe tapers is discussed and relevant examples are given to illustrate this. This discussion includes also aperiodic spaced planar array antennas.

Manuscript received First Publication; current version published xxxx xx, 2016.

The author, retired, was with the TNO Physics and Electronics Laboratory, The Hague, The Netherlands. He is now at Clinckenburgh 32, 2343 JH Oegstgeest, The Netherlands (e-mail: willkeizer@ieee.org).

Color version of one or more of the figures in this paper are available online at http://ieeexplor.ieee.org.

Digital Object Identifier

## II. Theory

In considering the synthesis of a low sidelobe taper it proves convenient to deal with the array factor rather the actual far-field that includes the embedded element pattern. The expression of the array factor AF in the far-field direction $(\theta, \varphi)$ of a rectangular planar phased antenna consisting of $N$ rows and $M$ columns of elements, arranged along a rectangular lattice with an element spacing $d_x$ in the X-direction and $d_y$ in the Y-direction, can be written as

$$AF(u,v) = \sum_{m=0}^{M-1} \sum_{n=0}^{N-1} A_{mn} e^{jk(md_x u + nd_y v)} \qquad (1)$$

where $A_{mn}$ the complex excitation of element $(m,n)$, $k$ is the wavenumber $(2\pi/\lambda)$ and $\lambda$ the operating wavelength.

While (1) represents a 2-D Fourier series and the array elements are arranged in a periodic grid, makes that AF is periodic in $u$-dimension over the interval $\lambda/d_x$ and periodic in $v$-dimension over the interval $\lambda/d_y$ (the dimensions of the grating lobe lattice in $u$-$v$ space). The rectangular region in $u$-$v$ space, covered by a single period or cell of $AF$ is given by $\{-0.5\lambda/d_x \leq u < 0.5\lambda/d_x$ and $-0.5\lambda/d_y \leq v < 0.5\lambda/d_y\}$. The periodicity of AF in $u$-$v$ space is responsible for the occurrence of grating lobes. These lobes can be become visible as more than one period of $AF$ fits into visible u-v space.

Because AF is a finite Fourier series, a number of Fourier properties apply to it. In the context of taper synthesis two Fourier properties are relevant: the shift property and the scale property. The expression for the Fourier shift operation is given in the Appendix by (6). When applying a linear phase taper to the element excitations across the aperture, the main beam is shifted over an angular distance that equals the slope of the linear phase taper. Main beam scanning corresponds to a linear transformation in the u-v space that does not affect the shape of the array factor. If the PSLL of AF in invisible u-v space does not differ from that in visible u-v space then scanning of the main beam does not degrade the PSLL of the visible part of AF.

The other Fourier property able to alter the PSLL of AF located in visible u-v space, is the scale property, (7) of the Appendix. Changing the operating frequency of an array antenna corresponds to the Fourier scale property. Such scaling modifies the angular width of all lobes in u-v space but

not their relative peak levels. When AF extends into invisible u-v space, a part of it can move into visible u-v space when the operating frequency is raised and can therefore increase the PSLL as the invading sidelobe region has a higher PSLL than that of the visible region before the beam was scanned.

The next section reveals the consequences when the synthesis of a phase-only taper or amplitude only taper is restricted to visible u-v space.

## III. SIMULATIONS

Fig. 1a shows the area of AF (yellow colored region) for a planar array with a 0.5λ square element grid at 10 GHz. Due to this element spacing, AF covers the area $\{-1 \le u < 1$ and $-1 \le v < 1\}$ and extends therefore for a substantial part into invisible u-v space. The grating lobes are indicated by the symbol *.

Fig. 1b shows the situation for AF when a low sidelobe taper synthesis is performed with the main beam at broadside and ignoring the invisible space part of AF. Under this circumstance the sidelobe behavior of the invisible part of AF is fully undefined and therefore also its PSLL. The white areas in Fig 1b represent the regions with undefined sidelobe behavior since these regions were excluded from the taper synthesis. Fig. 1c illustrates what happens when the main beam is scanned away from broadside to $\theta = 30^0$ in the plane $\varphi = 0^0$. Since two white areas with undefined PSLLs enter visible space, a degradation of the PSLL in visible u-v space cannot be excluded. A comparable situation occurs when the operating frequency is raised.

A phase-only taper has been synthesized for a planer array antenna with a circular aperture and equipped with 7788 isotropic elements featuring a square element grid with 0.5λ spacing at 10 GHz. The low sidelobe taper synthesis was restricted to visible u-v space and the PSLL requirement was -38.0 dB which requirement was met after 337 iterations.

Fig. 2a shows the far-field pattern when the beam is scanned $30^0$ away from broadside in the plane $\varphi = 0^0$. The corresponding distribution of the main and peak sidelobe levels is depicted in Fig. 2b. One can see that due to scanning of the main beam the PSLL increases from -38.0 dB to -15.6 dB. Note that the locations of the regions with a substantial increased PSLL confirm exactly with the predictions of Fig. 1c. The way the PSLL of the same antenna configuration of Fig. 2 degrades by only raising the frequency from 10 to 12 GHz without scanning the main beam, is illustrated by Fig. 3.

Fig. 4 shows how the PSLL and directivity (Dir) of the same array antenna vary when the beam is scanned away from broadside up to $\theta = 60^0$ in the plane $\varphi = 0^0$. At broadside the directivity is 40.2 dBi and drops substantially already at scan angle $\theta = 5^0$ while PSLL raises sharply with 18.4 dB compared to broadside scan position. At scan position $\theta = 60^0$ the directivity decreases to 33.6 dBi, a degradation of 6.6 dB compared to its value at broadside. The results in Fig. 4 refer to 10 GHz.

Table 1 summarizes the Dir and PSLL results of Fig 4 and includes also the directivity and PSLL findings at 12 GHz of

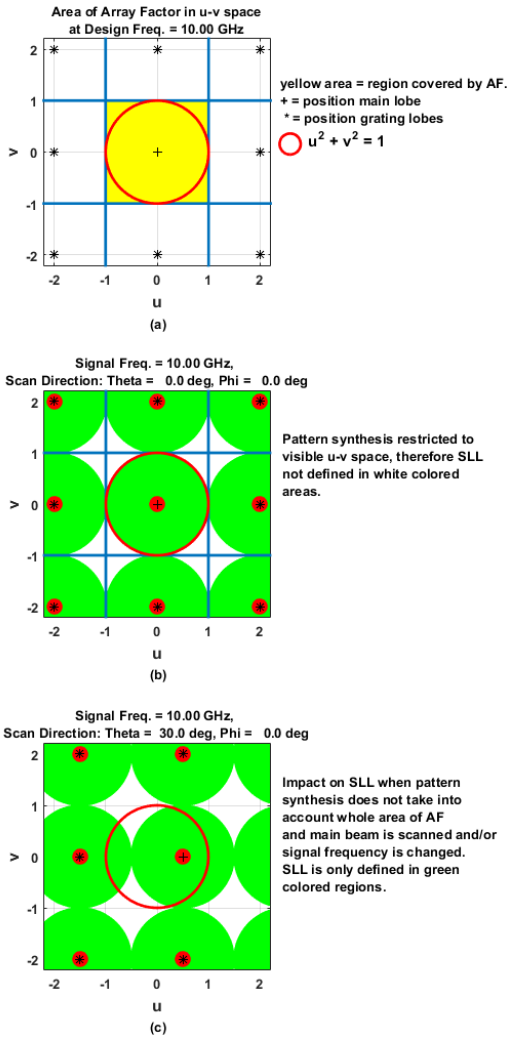


Fig. 1. (a) Area of AF in u-v space for square element grid with 0.5 λ element spacing. (b) Green colored areas indicate the regions for which the PSLL is defined when the synthesis is restricted to the part of AF located in visible u-v space. (c) Main beam scanned to $\theta = 30^0$ in the plane $\varphi = 0^0$ with the result that two white areas with undefined PSLL enter visible space.

Fig. 3. The 3 dB beamwidth values in this table illustrate that in accordance with the Fourier shift property the 3 dB beamwidth expressed in cosine direction coordinates is invariant with scan angle as long as the frequency is not changed. Fig. 5 shows the directivity and PSLL of the far-field results for the same 7788-element array when the synthesis of its phase-only taper involves the whole AF area in u-v space and the main beam is scanned. The phase-only taper was synthesized for a PSLL of -32.4 dB at 10 GHz and involved 855 iterations. The PSLL results in Fig. 5 demonstrate that the peak side lobe level is invariant with scan angle. Furthermore, that the decline of Dir for increasing scan angle is much smaller compared to the phase-only taper that involves only the visible u-v space part of *AF* during its synthesis. However also for this taper the drop in Dir with scan angle θ deviates from $\cos\theta$.

Table 2 summarizes the results of Fig. 5 and contains also the associated 3 dB beamwidth values including Dir and PSLL results at 12 GHz for the broadside beam. At 12 GHz the

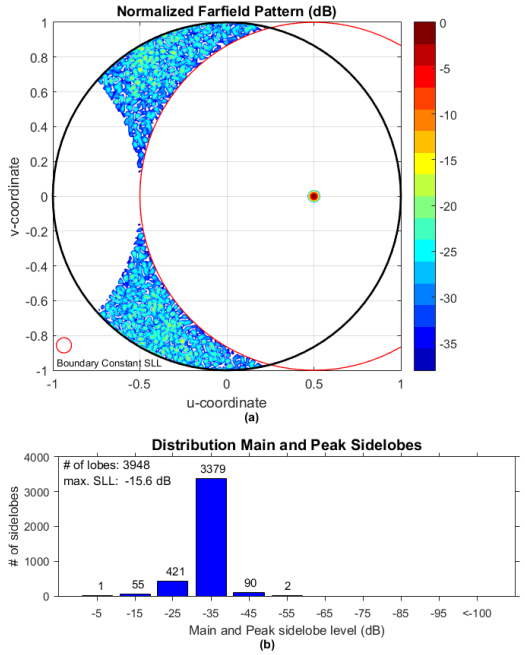


Fig. 2. Far-field results of the 7788 isotropic element circular planar array antenna at 10 GHz produced by a phase-only taper synthesized for only visible u-v space. This array features a square element grid with a 0.5λ spacing. The main beam is scanned to $\theta = 30^0$ in the plane $\varphi = 0^0$. (a) Pseudo contour plot of the far-field. (b) Associated distribution of the main beam and peak side lobe levels.

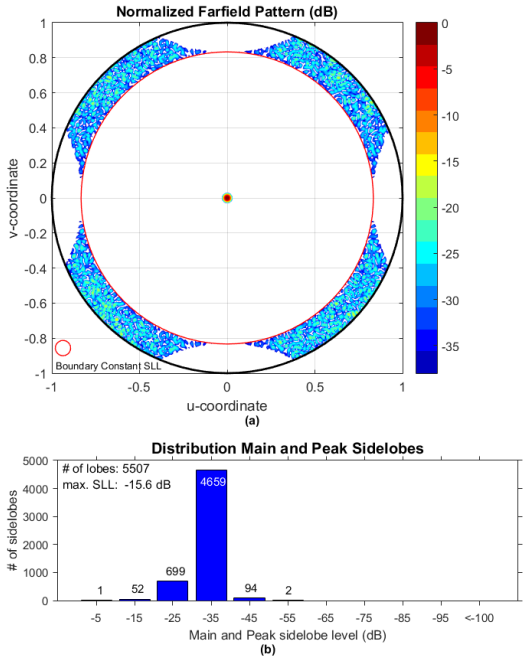


Fig. 3. Far-field results of the same planar array antenna of Fig. 1. (a) Pseudo contour plot of the far-field at 12 GHz and the main beam at broadside . (b) Associated distribution of the main beam and peak side lobe levels.

PSLL is still the same as those at 10 GHz in accordance with theory. A similar computation as done for the phase-only taper as described earlier in this paper, was also performed for a low sidelobe amplitude-only taper featuring a –60.4 dB PSLL requirement. The synthesis of the amplitude-only taper was restricted to visible space. Fig. 6 shows at 10 GHz the Dir and

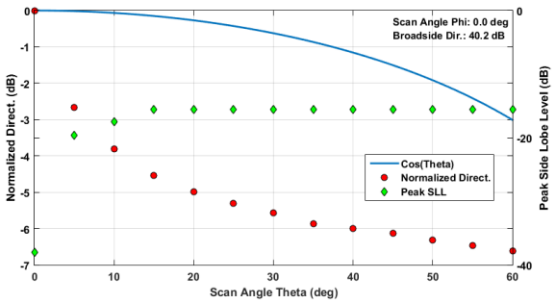


Fig. 4. Directivity and PSLL versus scan angle when the main beam is scanned away from broadside in the plane $\varphi = 0^0$ at 10 GHz. These results apply to a 7788-element planar array antenna having a circular aperture and with 0.5λ square grid spacing operating with a synthesized phase-only taper. The synthesis of this taper did not involve invisible u-v space.

TABLE 1.
OVERVIEW OF DIR AND PSLL RESULTS SHOWN IN FIG. 2 INCLUDING CORRESPONDING RESULTS WHEN THE FREQUENCY IS RAISED.

| Scan Direction (deg) | | Freq. (GHz) | Direct. (dBi) | PSLL (dB) | $u_{3dB}$ |
|---|---|---|---|---|---|
| Theta | Phi | | | | |
| 0 | 0 | 10 | 40.17 | -38.0 | 0.0263 |
| 5 | 0 | 10 | 37.51 | -19.6 | 0.0263 |
| 15 | 0 | 10 | 35.62 | -15.6 | 0.0263 |
| 30 | 0 | 10 | 34.06 | -15.6 | 0.0263 |
| 60 | 0 | 10 | 33.55 | -15.6 | 0.0263 |
| 0 | 0 | 12 | 34.26 | -15.6 | 0.0219 |

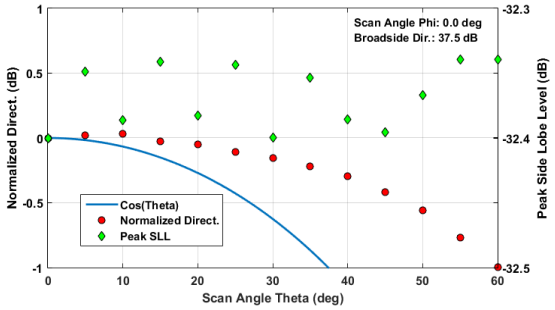


Fig. 5. Directivity and PSLL versus scan angle when the main beam is scanned away from broadside in the plane $\varphi = 0^0$ at 10 GHz. These results apply to the 7788 isotropic element planar array antenna with 0.5λ grid spacing operating with a synthesized phase-only taper involving the whole AF period in u-v space.

TABLE 2.
OVERVIEW OF DIR AND PSLL RESULTS SHOWN IN FIG. 5 INCLUDING CORRESPONDING RESULTS WHEN THE FREQUENCY IS RAISED.

| Scan Direction (deg) | | Freq. (GHz) | Direct. (dBi) | PSLL (dB) | $u_{3dB}$ |
|---|---|---|---|---|---|
| Theta | Phi | | | | |
| 0 | 0 | 10 | 37.47 | -32.4 | 0.0236 |
| 5 | 0 | 10 | 37.49 | -32.3 | 0.0236 |
| 15 | 0 | 10 | 37.44 | -32.3 | 0.0236 |
| 30 | 0 | 10 | 37.32 | -32.4 | 0.0236 |
| 60 | 0 | 10 | 36.47 | -32.3 | 0.0236 |
| 0 | 0 | 12 | 37.86 | -32.4 | 0.0196 |

PSLL results when the 7788 isotropic element array antenna with the square element grid operates with an amplitude-only taper synthesized for the visible u-v space part of *AF*. Identical to the phase-only taper synthesized for only visible space, scanning of the main beam induced an increase of PSLL from

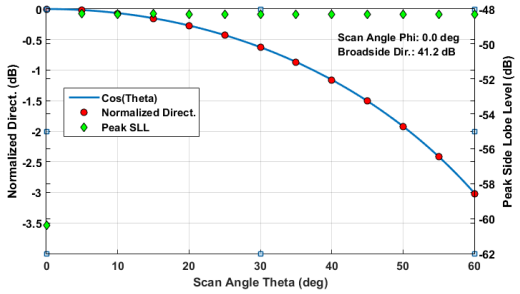


Fig. 6. Directivity and PSLL versus scan angle when the main beam is scanned away from broadside in the plane φ = $0^0$ at 10 GHz. These results apply to the 7788-element planar array antenna with 0.5λ grid spacing operating with a synthesized amplitude taper involving only the visible space period of AF.

-60 dB at broadside up to -48 dB for any other scan angle. The decrease of the directivity versus scan angle does not show any anomaly and confirms to $\cos\theta$.

Comparable results with respect to scan and frequency invariant tapers have been obtained for the same array using a triangular grid. The described approach can be applied to any array aperture shape, any array size and any periodic element grid. The only requirement for scan and frequency proof tapers is that an entire periodic cell of *AF* in *u-v* space must be involved in the taper synthesis. Relevant information on shape and dimensions of the AF cell in u-v space for periodic planar array antennas can be found in [1].

## IV. Directivity versus Scan Angle $\theta_o$

For a large planar array antenna the expression for the directivity versus scan angle $\theta_o$ can usually be approximated quite accurately by

$$Dir(u_o, v_o) \approx \frac{4\pi}{\lambda^2}\,\eta A_e \cos\theta_o \qquad (2)$$

where $\eta$ is the taper efficiency and $A_e$ the aperture size.

Expression (2) holds for any low sidelobe amplitude-only taper even for an uniform element distribution. As has been demonstrated, (2) is far from suited for calculating the directivity versus scan angle $\theta_o$for planar array antennas operating with phase-only tapers. Why this dependency is violated for phase-only tapers can be explained as follow.

The directivity for an array antenna when the main beam is scanned to the direction $(u_o, v_o)$ follows from [2]

$$Dir(u_o, v_o) = \frac{4\pi|F(u_o, v_o)|^2}{\iint_{u^2+v^2\le 1} \frac{|F(u,v|^2}{\sqrt{1-u^2-v^2}}\,dudv} \qquad (3)$$

where *F* is the array far-field.

For an array antenna having an isotropic embedded element pattern, $|F(u_o, v_o)|^2$ in (3) does not change when scanning the main beam. Also the far-field power content of the main beam will not vary with scan angle due to the Fourier shift property. For a large array antenna operating with an amplitude-only low-sidelobe taper, the power of the total radiated far-field will largely (>90%) be contained in the narrow main beam, [3]. Under this circumstance the integration of $|F(u,v|^2$ in the sidelobe region of visible u-v space hardly contributes to the numerator of (4) and needs therefore only involve the main beam width, null-to-null. Since $\sqrt{1-u^2-v^2}$ in (3) hardly varies over a narrow main beam, it can be replaced by $\sqrt{1-{u_o}^2-{v_o}^2} = \cos\theta_o$, subsequently taken out from the integral in the numerator of (3) and positioned in the denominator. In this way $\cos\theta_o$ becomes the only term in (3) that varies with scan angle.

With phase-only tapers, the sidelobe region in visible space contains a substantial portion of the total radiated power and can therefore not be neglected since the integration of $|F(u,v|^2$ must involve whole visible space. The fairly large sidelobe power content distorts not only the $\cos\theta$ dependency of the array directivity and but therefore also lowers it.

## V. Array Antennas with an Aperiodic Element Grid

The Fourier scan and shift properties (5) and (6) apply likewise to array factors of array antennas featuring an aperiodic element grid. Due to the aperiodic element locations the array factor extends always into invisible space. This means that the pattern synthesis of such an array must take into account the region of invisible u-v space that enters visible space when the main beam is scanned and/or the operating frequency is raised, otherwise an increase in PSLL is very likely. To get scan and frequency invariant tapers for planar array antennas with aperiodic element spacing, the taper or pattern synthesis has to performed over the region $u^2 + v^2 \le r^2$ with $r = (1+\sin\theta_m)\,f_H/f_o$ where $\theta_m$is the maximum scan angle, $f_H$ the highest frequency of operation and $f_o$ the synthesis frequency. This region requirement follows directly from (6) and (7).

In recent years various papers [4]-[9] have been published on the synthesis of linear arrays with aperiodic element spacing in order to get low sidelobe patterns for equal amplitude excitation. The majority of these designs make use of synthesis methods considering only visible space with the beam at broadside. Therefore, all these designs suffer from a large increase in PSLL when scanning the main beam. Calculations performed on the 14-element array of Fig. 4 in [4] with the beam scanned to $15^o$ reveals a -8.21 dB PSLL while at broadside the PSLL is -20.21 dB. A comparable increase in PSLL at scan angle $15^o$ was calculated for aperiodic linear array designs in [5]-[9].

A good exception was the non-uniformly spaced 21-element linear array of Fig. 4 in [10] of which the pattern synthesis was carried out over the range $-2 \le u \le 2$ to assure that the beam can be scanned amongst the two endfire directions. Realization of a good wideband design for the same scan range requirement was however not successful but could be obtained in a very simple way by extending the synthesis range to $-2cor \le u \le 2cor$ with $cor$ equal to $f_H/f_o$.

An illustrative example of the impact on directivity and PSLL when the invisible part of the array factor is excluded

from pattern synthesis for a planar array with aperiodic elements, is given by [11]. This paper describes the synthesis of Taylor like low sidelobe patterns for planar array antennas with uniformly excited elements positioned in concentric rings with non-uniform ring spacing. Since invisible space was excluded from the synthesis of these patterns, the designed array antennas suffer from a large loss in directivity 3.5 dB when scanning to $\theta_o = 15^0$ accompanied by large increase in peak level for the far-out sidelobes according to Fig. 6 in [11]. These results show a strong resemblance with the results of Fig. 4 in this communication.

## VI. Conclusion

This paper clarifies how to synthesize low sidelobe tapers for planar array antennas with a periodic element grid which are scan and frequency invariant with respect to PSLL. In order to realize such tapers for array antennas with a periodic element grid, it is essential that the synthesis involves a complete period of AF in u-v space. The tapers in [12]-[16] are all designed in this way.

For aperiodic array antennas an expression was given for the size of AF in u-v space to get scan and frequency invariant pattern designs with respect to PSLL.

It was shown that the directivity versus scan angle of planar array antennas operating with phase-only low sidelobe tapers violate the $\cos\theta$ dependency. It was also explained why.

All results presented in this paper have been calculated with the phased array simulator software APAS [2].

## Appendix

Equation (1) can be casted as

$$F(u',v') = \sum_{x=0}^{M-1}\sum_{y=0}^{N-1} f(x,y)e^{j2\pi(u'x/M+v'y/N)} \qquad (4)$$

which is the standard expression of the inverse 2-D DFT commonly used in literature. In (4) the parameter $F$ represents the array factor and $f(x,y)$ the aperture excitation. The DFT transform of (4) can be denoted by

$$F(u',v') \;\Leftrightarrow\; f(x,y) \qquad (5)$$

Since (4) is a 2-D DFT a number of Fourier properties apply to it such as the Fourier shift and scale property. The shift property is given by

$$F(u'-u'_o, v'-v'_o) \;\Leftrightarrow\; f(x,y)e^{j2\pi(u'_o x/M+v'_o y/N)} \qquad (6)$$

Scanning of the main beam of an array antenna confirms to (6). By applying a linear phase taper of the form $e^{j2\pi(u'_o x/M+v'_o y/N)}$ to the element excitations, the main beam is shifted to the direction $(u'_o, v'_o)$. This shift does not affect the amplitude of the scanned array factor and therefore also not the shape of the main beam.

The Fourier scale property is given by

$$F\left(\frac{u'}{a},\frac{v'}{b}\right) \;\Leftrightarrow\; \frac{1}{|ab|}f(ax,by) \qquad (7)$$

According to (7) expansion in the array aperture domain causes shrinking in u-v space. Such shrinking occurs when the operation frequency is raised since this affects the element grid dimensions normalized against operating wavelength.

## References


[1] Y. T. Lo, and S. W. Lee, "Affine transformation and its application to antenna array," *IEEE Trans. Antennas Propag*., vol. 13, pp. 890-896, Nov. 1965.

[2] W. P. M. N. Keizer, "APAS an advanced phased array simulator," *IEEE Antennas and Propag. Magazine*, vol. 52, no. 2, pp. 40-56, April 2010.

[3] R. C. Hansen, "Phased array antennas," John Wiley & Sons, Inc., New-York, 2001, pp. 115.

[4] R. L. Haupt, "Unit circle representation of aperiodic arrays," *IEEE Trans. Antennas Propag*., vol. 43, pp. 1152-1155, Oct. 1995.

[5] T. N. Kaifas, and J. N. Sahalos, "On the geometry synthesis of arrays with a given excitation by the orthogonal method,", *IEEE Trans. Antennas Propag*., vol. 56, pp. 3680-3688, Dec. 2008.

[6] P. Bevelacqua, and C. A. Balanis, "Minimum sidelobe levels for linear arrays,", *IEEE Trans. Antennas Propag*., vol. 55, pp. 3442-3449, Dec. 2007.

[7] O. M. Bucci, M. D'Urso, T. Isernia, P. Angeletti, and G. Tosso, "Deterministic synthesis of uniform amplitude sparse arrays via new density taper techniques," *IEEE Trans. Antennas Propag*., vol. 58, pp. 1949-1958, June 2010.

[8] E. Rajo-Iglesias, and Ò. Quevedo-Teruel, "Linear array synthesis using an ant-colony-optimization-based algorithm," *IEEE Antennas and Propag. Mag.*, vol. 49, pp. 70-79, April 2007.

[9] N. Jin, and Y. Rahmat-Samii, "Advances in particle swarm optimization for antenna designs: real number, binary, single-objective and multiobjective implementations," *IEEE Trans. Antennas Propag*., vol. 55, pp. 556-567, Mar. 2007.

[10] T. Isernia, F. J. Ares Pena, O. M. Bucci, M. D'Urso, J. Fondevila Gómez, and J. A. Rodríguez, "A hybrid approach for the optimal synthesis of pencil beams through array antennas," *IEEE Trans. Antennas Propag*., vol. 52, pp. 2912-2918, Nov. 2004.

[11] A.Á. Salas-Sánchez, J. A. Rodriguez-Gonzáles, E. Moreno-Piquero, and F.J. Ares-Pena, "Synthesis of Taylor-like patterns with uniformly excited multi-ring planar antennas," *IEEE Trans. Antennas Propag*., vol. 62, pp. 1589-1595, April 2014.

[12] W. P. M. N. Keizer, "Fast low-sidelobe synthesis for large planar array antennas utilizing successive Fourier transforms of the array factor," *IEEE Trans. Antennas Propag*., vol. 55, pp. 715-722, Mar. 2007.

[13] W. P. M. N. Keizer, "Element failure correction for a large monopulse phased array antenna with active amplitude weighting," *IEEE Trans. Antennas Propag.*, vol. 55, pp. 2211-2218, Aug. 2007.

[14] W. P. M. N. Keizer, "Synthesis of thinned planar circular and square arrays using density tapering," *IEEE Trans. Antennas Propag*., vol. 62, no. 4, Part 1, pp. 1555-1563, April 2014.

[15] W. P. M. N. Keizer, "Large planar array thinning using iterative FFT techniques," *IEEE Trans. Antennas Propag*., vol. 57, no. 10, pp. 3359-3362, Oct. 2009.

[16] W. P. M. N. Keizer, "Amplitude-only low sidelobe synthesis for large thinned planar array antennas," *IEEE Trans. Antennas Propag.*, vol. 60, pp. 1157-1161, Feb. 2012.